Switching-induced Turing instability

J. Buceta and Katja Lindenberg
Department of Chemistry and Biochemistry and Institute for Nonlinear Science, University of California, San Diego, 9500 Gilman Drive, La Jolla, California 92093-0340

(Received 16 April 2002; revised manuscript 18 July 2002; published 4 October 2002)

We propose a mechanism for inducing a Turing instability in systems whose only stable state is pattern-free and homogeneous. Global alternation between two dynamics, *each* of which has *the same* homogeneous stable state, may induce a Turing instability that leads to pattern formation. We determine what kind of alternation can drive the system to a Turing instability, and show that the appearance of the induced spatiotemporal structure depends on the ratio of two characteristic times, one determined by the external forcing and the other by the instability that drives the system at short times. The mechanism is illustrated by means of theoretical calculations and numerical simulations on two well-known biological models that are relevant in morphogenesis.

DOI: 10.1103/PhysRevE.66.046202 PACS number(s): 47.54.+r, 05.45.−a, 89.75.Kd

I. INTRODUCTION

Nonequilibrium patterns are ubiquitous in nature [1]. The discovery and understanding of new mechanisms for generating spatiotemporal structures is, therefore, a subject of interest and research in many fields of science. One such possible mechanism involves the forced alternation between two dynamics. The idea that dynamical switching might lead to interesting structures arose from a number of examples in which such alternation provokes unexpected results. The prototypical example is the Brownian flashing ratchet [2], where either periodic or random switching between two local potentials generates a current of particles in a system, where neither of the potentials alone produces a current. Another example occurs in the so-called Parrondo's paradox, where alternately playing two losing games produces a winning result (''paradoxical games'') [3]. An extension of this phenomenology to spatially distributed systems has recently been shown to lead to pattern formation [4]. In particular, working with models based on Swift-Hohenberg (SH)-type equations [5] we have shown that either periodic or random *global* switching between two dynamics may lead to stationary or oscillatory spatial patterns. That mechanism requires a key ingredient, the alternation between dynamics with two *different* stable homogeneous states. The resulting states depend on the relation between two competing characteristic time scales: One is the characteristic *switching time* $t_{\rm ext}$, which determines the length of time that the system spends evolving in each dynamic; the other is the time that the system takes to accommodate to a new dynamic upon switching, that is, the *relaxation time* t_r. When switching is slow ($t_{\rm ext} \gg t_r$), the system alternates between homogeneous states. If switching is sufficiently rapid ($t_{\rm ext} \ll t_r$), a new unstable equilibrium point arises, and stationary patterns develop. If the times are comparable ($t_{\rm ext} \sim t_r$) and the switching is periodic, oscillatory patterns develop.

Herein we propose an entirely different mechanism for pattern formation in reaction-diffusion systems [6], again induced by global alternation of dynamics but otherwise involving very different requirements and time scales than those described above. This mechanism applies even to systems where there is a *single unique* stable homogeneous state, i.e., one that is *the same* and pattern-free, for both of the alternating dynamics. Relaxation processes play no role in this mechanism. We will show that in this case collective effects and short time instabilities are responsible for developing heterogeneous structures. The mechanism, in that sense, resembles that of some noise-induced phase transitions [7,8], with the significant difference that in the latter the random perturbations must be local whereas in our case the system is driven globally.

The paper is organized as follows. In Sec. II we present a short introduction to reaction-diffusion systems and the so-called Turing instability [9], which plays an important role in biological models for morphogenesis, chemical reactions, and many others physicochemical systems [6]. In that section we also show that an initial instability that drives the system at short times can be consistent with a stable homogeneous state at long times. This combination is essential for our mechanism. Section III details how it is that global alternation of two reaction-diffusion dynamics that share a common equilibrium may lead to pattern formation. The internal time scale that determines whether or not patterns are produced is estimated in Sec. IV. Two reaction-diffusion systems frequently invoked in biological contexts are presented in Sec. V, and parameter ranges that lead to morphogenesis by dynamic alternation in these two systems are determined. Numerical simulations confirming these conditions are presented for one of the two models (the activator-substrate model) in Sec. VI, where we show examples of the formation of stationary patterns and of oscillatory patterns. Finally, in Sec. VII we summarize our main conclusions and indicate some possible future directions.

II. REACTION-DIFFUSION SYSTEMS

Consider a simple reaction-diffusion system, where two species interact. The concentrations of the two species at space point $\mathbf{r}$ and time t are $u=u(\mathbf{r},t)$ and $v=v(\mathbf{r},t)$, and their evolution equations are

$$\partial_t u = f(u,v) + D_u \nabla^2 u,$$

$$\partial_t v = g(u,v) + D_v \nabla^2 v. \qquad (1)$$

A steady state occurs at concentrations u^s and v^s such that

$$f(u^s,v^s)=g(u^s,v^s)=0. \tag{2}$$

Its stability can be established by means of a linear perturbation analysis of small perturbations about the steady state,

$$u=u^s+\delta u, \quad v=v^s+\delta v, \tag{3}$$

and linearization of f and g around the equilibrium point. We find the following evolution equation for the perturbations δu and δv:

$$\partial_t\begin{pmatrix}\delta u\\ \delta v\end{pmatrix}=\begin{pmatrix}f_u+D_u\nabla^2 & f_v\\ g_u & g_v+D_v\nabla^2\end{pmatrix}\begin{pmatrix}\delta u\\ \delta v\end{pmatrix}, \tag{4}$$

where

$$f_z\equiv\partial_z f(u,v)|_{(u^s,v^s)}, \quad g_z\equiv\partial_z g(u,v)|_{(u^s,v^s)}, \tag{5}$$

and z stands for u or v. The solution is a linear combination of plane waves,

$$\delta u(\mathbf{r},t)=\sum_{\mathbf{q}}\ \delta u_{\mathbf{q}}(t)\cos(\mathbf{q}\cdot\mathbf{r}),$$

$$\delta v(\mathbf{r},t)=\sum_{\mathbf{q}}\ \delta v_{\mathbf{q}}(t)\cos(\mathbf{q}\cdot\mathbf{r}), \tag{6}$$

where the amplitudes of the waves with wave vector $\mathbf{q}$ satisfy the following equation:

$$\partial_t\mathbf{Z}_{\mathbf{q}}=\mathbb{J}_{\mathbf{q}}\mathbf{Z}_{\mathbf{q}}. \tag{7}$$

Here

$$\mathbf{Z}_{\mathbf{q}}=\begin{pmatrix}\delta u_{\mathbf{q}}\\ \delta v_{\mathbf{q}}\end{pmatrix}, \quad \mathbb{J}_{\mathbf{q}}=\begin{pmatrix}f_u-q^2D_u & f_v\\ g_u & g_v-q^2D_v\end{pmatrix}. \tag{8}$$

The formal solution of Eq. (7) is

$$\mathbf{Z}_q(t)=\mathbf{Z}_q(0)\exp(\mathbb{J}_q t). \tag{9}$$

We have replaced the vectorial subscripts $\mathbf{q}$ by the magnitude q because the evolution operator $\mathbb{J}$ retains q-spherically-symmetric initial conditions, to which we restrict ourselves. The real parts of the eigenvalues $s(q)$ of the operator $\mathbb{J}_q$ determine whether a perturbation diverges $[\mathrm{Re}(s(q))>0]$ or decays to zero $[\mathrm{Re}(s(q))<0]$. The eigenvalues obey the equation

$$s^2(q)-s(q)\mathrm{Tr}(\mathbb{J}_q)+\mathrm{Det}(\mathbb{J}_q)=0. \tag{10}$$

The fixed point (u^s,v^s) is stable with respect to *homogeneous* perturbations if $\mathrm{Tr}(\mathbb{J}_0)<0$ and $\mathrm{Det}(\mathbb{J}_0)>0$. Moreover, an *inhomogeneous* perturbation with wave vector $q\neq 0$ decays if $\mathrm{Tr}(\mathbb{J}_q)<0$ and $\mathrm{Det}(\mathbb{J}_q)>0$. These conditions can be translated to the following sufficient, but not necessary, conditions for the stability of the fixed point with respect to *homogeneous and inhomogeneous* perturbations:

$$f_u+g_v<0, \tag{11}$$

$$f_u g_v-f_v g_u>0, \tag{12}$$

$$D_u g_v+D_v f_u<0. \tag{13}$$

On the other hand a steady state will be unstable with respect to some *inhomogeneous* perturbations (but stable against homogeneous perturbations) if condition (13) is replaced by

$$D_u g_v+D_v f_u>2[D_u D_v(f_u g_v-f_v g_u)]^{1/2}. \tag{14}$$

The latter case is known as the *Turing instability* and leads to the development of a pattern [9]. The wave vector q^* of the spatial structure is that which maximizes $s(q)$.

If a homogeneous state is stable, Eqs. (11) and (13) forbid both f_u *and* g_v to be simultaneously positive. However, none of the stability conditions reject the possibility that $f_u g_v<0$. Moreover, if $f_u g_v<0$ then, by Eq. (12), $f_v g_u<0$. We also point out that at short times the evolution is dictated by the signs of the individual terms f and g. Therefore, it is possible that even when a homogeneous state is stable, one field (or both) may present an instability at short temporal scales independently of the initial condition. That instability will drive the system up to time scales of order $O(1/\max\{f_u,f_v,g_u,g_v\})$ and is crucial in the proposed mechanism of pattern formation, as shown below. Note that in the case of single-field dynamics, as in the SH model, if a homogeneous state is stable it is not possible for the system to present such a short time instability. As a consequence, the mechanism of pattern formation by the alternation of dynamics proposed below applies only to *multifield* systems, and is completely different from that recently proposed for single-field systems based on relaxation processes [4].

III. ALTERNATION OF DYNAMICS

Suppose that we globally alternate two reaction-diffusion dynamics in time. By ''globally'' we mean that at any given time *all* space points are driven by the same dynamic, that is, the reaction functions f and g and the diffusion coefficients D_u and D_v are not allowed to change from point to point. Moreover, let us consider two dynamics each of which by itself evolves to *the same* stable homogeneous equilibrium state. The question we wish to explore is whether it is possible to induce a Turing instability by global alternation of two such dynamics. Two points are clear even before further exploration: (i) For an instability to develop, it is necessary that the alternation process change the stability properties of the equilibrium state and (ii) Relaxation processes between equilibrium states play no role here since the two separate dynamics have the same equilibrium point.

Even though relaxation processes play no role in this discussion, there are nevertheless two temporal scales involved in the problem. One is the switching time t_{ext} that characterizes the externally imposed alternation of dynamics, and the other is an internal time t_{int} determined by the system dynamics. Clearly, the external time is the average time the system spends in each dynamic. In the case of pure periodic

switching $t_{\rm ext}=T/2$, where T is the period of the alternation process. If the switching process is random and switching between dynamics occurs with equal probability, its correlation function might be [10]

$$\mathcal{C}(t,t')=\exp(-|t-t'|/\tau), \tag{15}$$

where τ is the correlation time of the switching process. In this case $t_{\rm ext}=2\tau$.

Pattern formation requires an early-time instability that is ''captured'' by the alternation process. The internal time of interest turns out to be $t_{\rm int}\sim O(1/\max\{f_u,f_v,g_u,g_v\})$, that is, the time scale over which this early instability drives the evolution of the system. As mentioned earlier, such a time scale is also responsible for some noise-induced phase transition phenomena. However, contrary to the case here, in the noise-induced phenomena the noise acts *locally*. We will estimate the internal time in more detail in the following section.

The control parameter $r=t_{\rm ext}/t_{\rm int}$ separates slow and fast dynamics. When the alternation is slow, $r\gg 1$, no destabilization of the equilibrium point can be achieved since both dynamics drive the system to the *same* steady state, and, once there, the switching process can not move the system away from that state. Pattern formation can occur if the switching mechanism is sufficiently rapid, $r\ll 1$. Moreover, we will show that if $r\approx 1$ a resonance phenomenon that leads to oscillatory patterns occurs in the case of periodic alternation.

It is possible to establish rather general conditions under which pattern formation will or will not occur. Let the two dynamics be denoted by subscripts $i=1,2$, so that D_{iu}, D_{iv}, $f_i(u,v)$, and $g_i(u,v)$ denote the constants and functions under dynamic i. Each dynamic separately must satisfy the stability conditions (11)–(13). On the other hand, when dynamic alternation is very rapid ($r\ll 1$), adiabatic elimination immediately leads to the conclusion that the evolution of the system is driven by the *average* values $A_+\equiv\frac{1}{2}(A_1+A_2)$, where A stands for D_u, D_v, $f(u,v)$, and $g(u,v)$. An instability then occurs if the condition (13) is replaced by (14) for this average dynamic. A number of alternation schemes can easily be ascertained *not* to satisfy the necessary criteria. In particular, the diffusion and the reaction functions must both be alternated. A particularly simple alternation scheme that induces spatiotemporal patterns is

$$f_i(u,v)=a_i f(u,v),\quad g_i(u,v)=g(u,v),$$
$$D_{iu}=D_u,\quad D_{iv}=b_i D_v, \tag{16}$$

where the a_i and b_i are positive constants. Note that the coefficients in this alternation scheme can in principle be related to the presence or absence of an immobile complexing agent [6].

IV. ESTIMATION OF THE INTERNAL TIME

In the remainder of this paper we focus on the case of periodic alternation. In this section we provide a more detailed estimation of the time $t_{\rm int}$. We define the time $t=0$ to be the start of the alternation process. The evolution operator $\exp(\mathbb{J}_q t)$ in Eq. (9) is a product of successive evolution operators appropriate to each of the alternating dynamics. For instance, if we begin with dynamic 1 then at the end of n periods of alternation we have

$$\mathbf{Z}_q(nT)=\left[\exp\left(\mathbb{J}_q^1\frac{T}{2}\right)\exp\left(\mathbb{J}_q^2\frac{T}{2}\right)\right]^n\mathbf{Z}_q(0)=[\mathbb{G}_q(T)]^n\mathbf{Z}_q(0), \tag{17}$$

where the meaning of the notation $\mathbb{J}_q^i$ is obvious. Thus, the real parts of the eigenvalues of $\mathbb{G}_q(T)$ determine the stability of the alternation process. Note that the eigenvalues are the same whether one starts with either dynamic 1 or dynamic 2. Moreover, the eigenvalues are of course independent of the initial condition. The characteristic polynomial for the eigenvalues $\Lambda_q(T)$ of the operator $\mathbb{G}_q(T)$ is given by

$$\Lambda_q^2(T)-\Lambda_q(T)\mathrm{Tr}[\mathbb{G}_q(T)]+\mathrm{Det}[\mathbb{G}_q(T)]=0. \tag{18}$$

If $\mathrm{Re}(\Lambda_q(T))>1$ (<1) the alternation process leads to destabilization (stabilization) of the initial instability. Therefore, the condition $\mathrm{Re}(\Lambda_q(T))=1$ determines the critical stability curve.

When the alternation of dynamics does produce a Turing instability, there exists a critical value of the period, $\tilde{T}$, such that there are no instabilities for dynamic alternations slower than this critical period. Thus for all periods longer than $\tilde{T}$ the maxima of $\mathrm{Re}(\Lambda_q(T))$ as a function of q take values smaller than unity. The value $q=\tilde{q}$ associated with this instability is found from the conditions

$$\mathrm{Re}\Lambda_{\tilde{q}}(\tilde{T})=1,\quad \frac{\partial \mathrm{Re}\Lambda_q(\tilde{T})}{\partial q}\Big|_{q=\tilde{q}}=0. \tag{19}$$

We define the internal time $t_{\rm int}$ as half the value of the critical period $\tilde{T}$:

$$t_{int}\equiv\frac{\tilde{T}}{2}. \tag{20}$$

A Turing instability develops for any $T<\tilde{T}$ at the wave vector q^* that maximizes $\mathrm{Re}(\Lambda_q(T))$. In the limit $T\to 0$, the most unstable mode coincides with the one obtained by maximizing the eigenvalue $s(q)$ using the *effective* average dynamic.

V. MORPHOGENESIS

Because of their broad applicability to spatial differentiation [1,11], we select two specific reaction-diffusion models to illustrate the mechanism. In its most elementary variants, and in convenient dimensionless units, the activator-substrate [12] and activator-inhibitor [13] models read, respectively,

$$\partial_t u=a(u^2v-u)+\nabla^2 u,$$
$$\partial_t v=(1-u^2v)+D\nabla^2 v, \tag{21}$$

and

$$\partial_t u = a\left(\frac{u^2}{v} - u\right) + \nabla^2 u,$$

$$\partial_t v = (u^2 - v) + D\nabla^2 v. \tag{22}$$

The activator-substrate model (21) has been used to describe pigmentation patterns in sea shells [12,14], as well as the ontogeny of ribbing on ammonoid shells [15]. The variable v in this model can be interpreted as a substrate being consumed by an activator u. On the other hand, the activator-inhibitor model (22) plays an important role in the understanding of the regeneration and transplantation of the hydra [13]. Here u and v represent, respectively, the concentration of an activator and of its antagonist, an inhibitor. In both models a denotes a (positive) cross-reaction coefficient, and both share the unique fixed point $u^s = v^s = 1$. This stationary state is independent of the values of a and D, although the values of these parameters determine its stability.

We set $D_{iu} = 1$ and define $D_i = b_i D_v$. Global alternation between two sets of constants $\{a_i, D_i\}$ obeying the following conditions leads to a Turing instability in each of the two models:

$$a_i < 1, \tag{23}$$

$$a_i D_i < 1, \tag{24}$$

$$(a_1 + a_2)(D_1 + D_2) > 2, \tag{25}$$

$$(a_1 + a_2)(D_1 + D_2) < 4(3 - 2\sqrt{2}),$$

or

$$(a_1 + a_2)(D_1 + D_2) > 4(3 + 2\sqrt{2}). \tag{26}$$

We stress again that for either of the sets $\{a_i, D_i\}$ by itself, the fixed point $u_s = v_s = 1$ is stable. If the "greater than" condition is chosen in Eq. (26), the inequality (25) is automatically fulfilled. One possible family of solutions of Eqs. (23)–(26) is

$$a_1 < 1, \tag{27}$$

$$a_2 < a_1\left(\frac{8\sqrt{2} - 11}{7}\right), \tag{28}$$

$$D_1 < \frac{1}{a_1}, \tag{29}$$

$$\frac{8\sqrt{2} + 12}{a_1 + a_2} - D_1 < D_2 < \frac{1}{a_2}. \tag{30}$$

VI. NUMERICAL SIMULATIONS

Two particular pairs of constants fulfilling the conditions (27)–(30) are $(a_1, D_1) = (\frac{3}{4}, 1)$ and $(a_2, D_2) = (\frac{3}{100}, 30)$. We use these values in Fig. 1, where we depict the loci

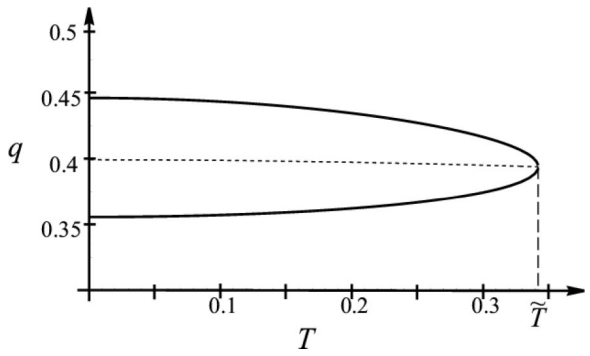

FIG. 1. For the two models described in the text, an alternation process with $T \leqslant \tilde{T}$ leads to pattern formation due to the destabilization of all the Fourier modes inside the solid curve. All points inside the solid curve represent unstable modes. The dashed line marks the most unstable mode of the patterns that develop for each T. The tip of the curve is at the critical period $\tilde{T} \simeq 0.34$ that defines the internal time $t_{int} = \tilde{T}/2$ and the associated wave vector $\tilde{q} = 0.393$. At $T = 0$ the most unstable mode occurs at $q^* = 0.399$.

$\mathrm{Re}(\Lambda_q(T)) = 1$ (solid curve), and the most unstable Fourier mode as a function of the alternation period, $q^*(T)$ (dotted line). An alternation process with $T \leqslant \tilde{T}$ leads to a Turing instability due to the destabilization of all the Fourier modes inside the solid curve. The resulting pattern will present a wavelength $\lambda(T) = 2\pi/q^*(T)$. The *tip* of the loci $\mathrm{Re}(\Lambda_q(T)) = 1$ determines the internal time $t_{\mathrm{int}} = \tilde{T}/2 \simeq 0.17$. Note that q^* is almost independent of T. Recall that Fig. 1 applies to *both* the activator-substrate model and the activator-inhibitor model.

We carry out numerical simulations of the activator-substrate model (21) on a 64×64 square lattice using a second order Runge-Kutta scheme with periodic boundary conditions [results for the model (22) are very similar]. The initial conditions for the concentrations of the species u and v are random. The space and time integration intervals are set to $\Delta t = 10^{-3}$ and $\Delta x = \Delta y = 1$. Since $\lambda \simeq 0.4$, we expect $L/\lambda \sim 4$ pattern wavelengths. We focus on the periodic alternation for different values of the ratio

$$r = \frac{T}{2t_{int}} = \frac{T}{\tilde{T}} \tag{31}$$

that controls the appearance of the Turing instability. When $r > 1$ we obtain a homogeneous state with concentrations $u^s = 1$, $v^s = 1$, as expected. As r decreases a Turing instability develops. In the limit $r \to 0$ a stationary pattern appears, as shown in Fig. 2. The stationary values of the concentration fields of u and v are shown by means of gray-scale density plots. Note the hexagonal structure of the Turing patterns, as well as the *negative* aspect of the concentrations, that is, in the regions where the activator u is highly concentrated, the substrate v has a low concentration. This behavior is expected since the activator grows by depleting the substrate. A spatial Fourier analysis of Fig. 2, shown in Fig. 3, reveals the most unstable mode of the pattern. The figure shows the spatial power spectrum of the concentration fields averaged over angles. This angle-averaged spectrum is appropriate because of the rotational symmetry of the concentration fields

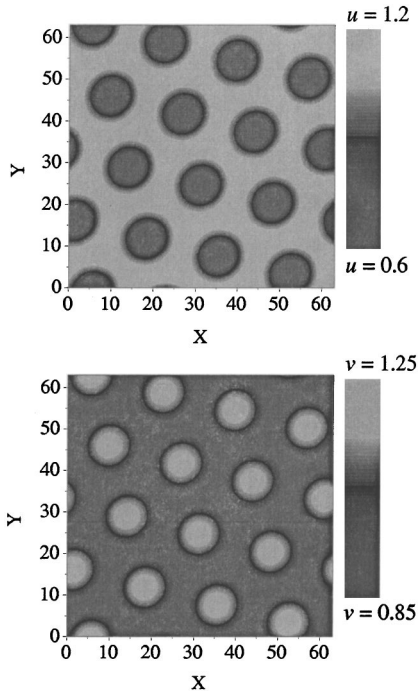

FIG. 2. Gray-scale density plot of the stationary concentrations of the chemical species u (activator) and v (substrate) for $r \simeq 0.03$.

$u(\mathbf{r})$ and $v(\mathbf{r})$. The most unstable mode is $q^* \simeq 0.4$, in agreement with the theoretical estimate.

A striking phenomenon occurs when the control parameter reaches values of order $r \sim 1$. A resonance between the two characteristic times leads to oscillatory patterns. Figure 4 shows the oscillatory pattern obtained for the concentration v for $r \simeq 0.9$. The spatial arrangement of the oscillatory pattern, as well as the most unstable mode, coincide with those obtained in the stationary case. We point out the analogy between these localized oscillations in the concentration of the morphogen v and the so-called *oscillons* found in vibrated granular layers [16].

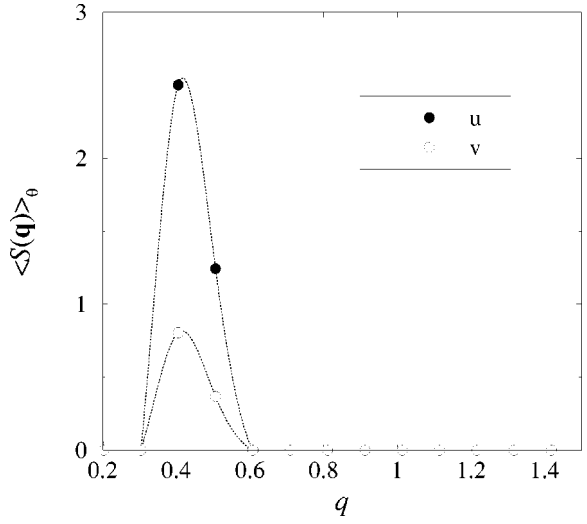

FIG. 3. Power spectrum of the concentration fields shown in Fig. 2 averaged over angles. The most unstable Fourier mode is $q^* \simeq 0.4$, in agreement with the theoretical estimate of Fig. 1.

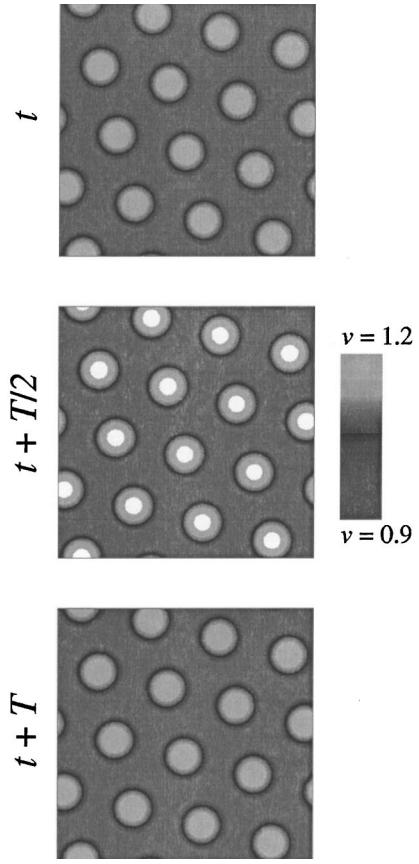

FIG. 4. Oscillatory pattern for the activator-substrate model with $r \simeq 0.9$. Snapshots of the concentration of the substrate v during a period of the alternation process. Note the localized oscillations arranged in a hexagonal structure.

VII. DISCUSSION AND CONCLUSIONS

We have shown how a nonequilibrium process of *global* alternation of dynamics may lead to pattern formation in reaction-diffusion systems, and we have used two particular models of biological interest to illustrate the necessary conditions for pattern formation and the actual patterns that may occur. To our knowledge, the mechanism is different from any other known pattern formation mechanism associated with dynamic alternation, because (i) the alternation is global (rather than spatially random), and (ii) the alternation can occur between two dynamics that share *a common* unique stable homogeneous equilibrium point when either acts alone. Nevertheless, a Turing instability develops when switching between these dynamics is sufficiently rapid.

Clearly, since the two dynamics may even share an equilibrium point, the mechanism leading to pattern formation does not involve relaxation processes from one equilibrium state to another [4]. Instead, the triggering mechanism in this case is the instability that may drive multifield systems at short times. We also noted that the occurrence of a Turing instability requires the alternation of both the reaction and

the diffusion terms in the field equations.

We presented a general class of reaction-diffusion systems where a Turing instability can be induced, and established sufficient conditions within this class for the occurrence of patterns. To illustrate the mechanism we chose two models well-known in a biological context, namely, the activator-substrate model [13] and the activator-inhibitor model [14]. While it may be difficult to implement in practice the global variations in these particular models, they serve as a feasibility study of the idea. Reaction-diffusion models in which natural periodic variations in the reaction and diffusion terms may occur arise in the context of epidemics studies in systems subject to seasonal variations, see, e.g., Ref. [17]. To support our theoretical description, we performed numerical simulations on the activator-inhibitor model and found excellent agreement with our predictions concerning relevant time scales. The control parameter for the mechanism is the ratio r of the alternation period and the time scale over which the early instability drives the evolution of the system. We showed that there are three different regimes of behavior depending on the value of the control parameter r. When $r \gg 1$ (slow alternation), the system relaxes to the unique stable equilibrium point of each of the two dynamics. When $r \ll 1$ (fast switching), an effective average dynamic drives the system and produces a Turing instability that leads to stationary pattern formation. Finally, if $r \approx 1$, a resonance phenomenon leads to oscillatory patterns. The oscillatory behavior is only observed for periodic alternation, whereas stationary pattern formation occurs with fast alternation whether the switching is periodic or random [4].

The work presented here concerns the dynamics alternation-induced destabilization of a unique stable equilibrium point, turning it into an unstable focus or an unstable node. One can of course envision destabilization processes that generate other equally interesting outcomes such as a Hopf bifurcation. As for the switching mechanism discussed herein, we note that the essential ingredient for pattern formation is an initial instability, and that the pattern formation process is more robust against changes in the alternation period the longer is the temporal window during which this instability drives the system. Clearly, dichotomous switching is not a fundamental component of the process. Other modulations should lead to the same phenomenology. Work on these questions is in progress.

ACKNOWLEDGMENTS

This work was supported by the Engineering Research Program of the Office of Basic Energy Sciences at the U. S. Department of Energy under Grant No. DE-FG03-86ER13606. Support was also provided by a grant from the University of California Institute for Mexico and the United States (UC MEXUS) and the Consejo Nacional de Ciencia y Tecnología de México (CONACYT), by MECD-Spain Grant No. EX2001-02880680, and by MCYT-Spain Grant No. BFM 2001-0291.

[1] M.C. Cross and P.C. Hohenberg, Rev. Mod. Phys. **65**, 851 (1993).
[2] R.D. Astumian and M. Bier, Phys. Rev. Lett. **72**, 1766 (1994).
[3] G.P. Harmer and D. Abbott, Sci. Sin. **14**, 206 (1999); Nature (London) **402**, 864 (1999); J.M.R. Parrondo, G.P. Harmer, and D. Abbott, Phys. Rev. Lett. **85**, 5226 (2000).
[4] J. Buceta, K. Lindenberg, and J.M.R. Parrondo, Phys. Rev. Lett. **88**, 024103 (2002); Phys. Rev. E (to be published); Fluct. Noise Lett. **2**, L21 (2002).
[5] J. Swift and P.C. Hohenberg, Phys. Rev. A **15**, 319 (1977).
[6] I.R. Epstein and J.A. Pojman, *An Introduction to Nonlinear Chemical Dynamics* (Oxford, New York, 1998).
[7] J. García-Ojalvo and J.M. Sancho, *Noise in Spatially Extended Systems* (Springer, New York, 1999); C. Van den Broeck, J.M.R. Parrondo, R. Toral, and R. Kawai, Phys. Rev. E **55**, 4084 (1997).
[8] J.M.R. Parrondo, C. Van den Broeck, J. Buceta, and F.J. de la Rubia, Physica A **224**, 153 (1996).
[9] A.M. Turing, Philos. Trans. R. Soc. London, Ser. B **B 237**, 37 (1952).
[10] C.W. Gardiner, *Handbook of Stochastic Methods*, 2nd ed. (Springer-Verlag, Berlin, 1985).
[11] A.J. Koch and H. Meinhardt, Rev. Mod. Phys. **66**, 1481 (1994); H. Meinhardt, *Models of Biological Pattern Formation* (Academic, New York, 1982).
[12] H. Meinhardt, J. Embryol. Exp. Morphol. **83**, 289 (1984); H. Meinhardt and M. Kingler, J. Theo. Biol. **126**, 63 (1987).
[13] A. Gierer and H. Meinhardt, Kybernetik **12**, 30 (1972).
[14] H. Meinhardt, *The Algorithmic Beauty of Sea Shells* (Springer, New York, 1998).
[15] Ø. Hammer and H. Bucher, Geo Bios **32**, 841 (1999).
[16] P.B. Umbanhowar, F. Melo, and H.L. Swinney, Nature (London) **382**, 793 (1996).
[17] G. Abramson and V.M. Kenkre, Phys. Rev. E **66**, 011912 (2002).